AALBORG UNIVERSITET

Identification of adipose stem cells subsets by the use of polychromatic flow cytometry

Aalborg University
May 29th 2020

Author
Martyna Duda

Supervisor
Vladimir Zachar

Medicine with industrial specialization
Biomedicine, Master Thesis
Department of Health Science and Technology

Aalborg University
Frederik Bajers Vej 7
9220 Aalborg, Denmark

Project title
Identification of adipose stem cells subsets
by the use of polychromatic
flow cytometry

Project period
September 1st 2019 to May 29th 2020

Project group
19gr9058

Supervisors
Vladimir Zachar

Author

_____
Martyna Duda, 20181347

Number of pages: 33

Number of standard pages: 25,3

Number of appendices: 2

Table of content

Abbreviations

ADSCs- adipose-derived stem cells

AIDS- acquired immune deficiency syndrome

ALCAM- activated leukocyte cell adhesion molecule

BAT- brown adipose tissue

BM-MSCs- bone marrow mesenchymal stem cells

DNA- deoxyribonucleic acid

FMO- fluorescence minus one

FBS- fetal bovine serum

FVS570- fixable viability stain 570

GFP- green fluorescent protein

HIV- human immunodeficiency virus

ISCT- the International Society for Cellular Therapy

PD-L1- programmed death ligand 1

PBS- phosphate-buffered saline

PMTs- photomultiplier tubes

SD- standard deviation

QC- quality control

scRNA-seq- single-cell RNA sequencing

SVF- stromal vascular fraction

WAT- white adipose tissue

Abstract

Background: Better understanding of phenotype profiling and functionality of adipose stem cells subsets may significantly improve stem cell treatment. Previous studies identified and sorted out populations with co-expression of four and six markers with diverse expression pattern. Among typical mesenchymal stem cell markers CD73+CD90+CD105+ other markers primarily associated with adipogenesis, osteogenesis, chondrogenesis, wound healing and immodulatory properties were examined. This study aims to identify expression profiles of five and eight co-expressed markers in two panels by the use of polychromatic flow cytometry. Additionally, stem cell were analyzed according to their culturing method- in a regular culture flask or in a bioreactor.

Method: Cells were isolated and seeded in flasks and in perfusion system of bioreactor. After reaching confluency, the cells were stained with viability dye and fluorochrome-conjugated antibodies. Flow cytometry was used in order to establish the marker profile. The data was then analyzed by implementing gating strategy.

Results: Four promising subsets with stable or rising expression upon culture were identified in this study. The study has proven divers expression profiles upon culture which was stated by previous study. Conversely to existing studies, the expression of CD34+ was found to be either low or non-existing.

Conclusions: Although further investigation and functional testing are needed, acquired in this project co-expression patterns may become a promising tool in personalized medicine and clinical treatment. As being a part of investigation research, more markers and methods may be implemented in order to establish subpopulation profiles and their best suitable application.

Key words: adipose-derived stem cells, polychromatic flow cytometry, immunophenotypic profile, subpopulations

1. Introduction

In recent years stem cells have shown the clinical utility in areas such as regenerative medicine and wound repair, cell-based therapy, and cancer research. Especially, adipose-derived stem cells (ADSCs) have gained a lot of attention due to their abundance in human body, high cell yield as well as strong proliferation capacity [1] Main interest of ADSCs is focused on their composition. As previous studies confirmed high heterogeneity among stem cells populations, it is likely that there is a connection between composition of stem cells population and its clinical value. Therefore, it is crucial to have a full characterization of stem cells prior to the development of a clinical standardization. [2] By the phenotypic analysis, different subpopulations of ADSCs can be separated and as a result each subpopulation can be tested for its precise therapeutic application. This study was to identify phenotypic subsets with different marker profiles using multichromatic flow cytometry. Simultaneously, the study intends to compare marker profiles of populations growing in an adherent culture in a culture bottles to populations growing in a bioreactor.

1.1. Mesenchymal stem cells (MSCs)

When categorized by their potency, stem cells can be divided into unipotent (able to give rise to only one cell type), totipotent (able to give rise to any cell type or a complete embryo), pluripotent (able to give rise to several different cell types), multipotent (able to give rise to multiple cell types) and oligopotent (able to give rise to closely related cell types, e.g. a lymphoid cell can create a B- or T-cell but not a red blood cell). Additionally, they can be classified either as embryonic, when they have been isolated from an inner cell mass of a blastocyst; somatic or adult, when they are isolated from a child or an adult; induced pluripotent, when they are generated from a somatic stem cell. [3] The formation of specific kinds of stem cells was pictured in Figure 1.

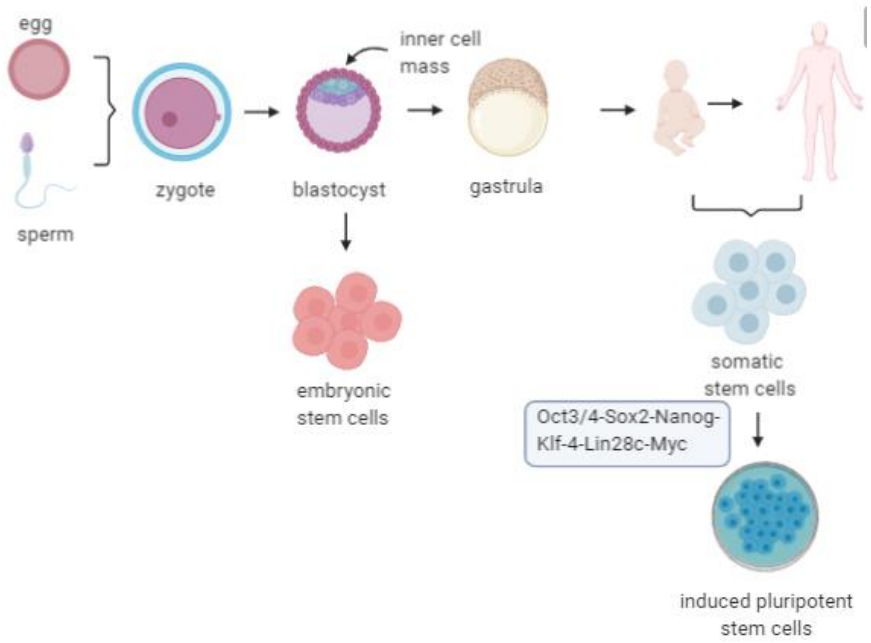

Figure 1. The diagram shows how different human stem cells are being produced during life time. As can be seen embryonic stem cells have their origin in the inner cell mass of the blastocyst. After birth and during adult life the body is producing somatic stem cells. When the cells are being induced with external factors it is possible to create induced pluripotent stem cells.

Up to the present time, a huge role is assigned to MSCs- multipotent, somatic stem cells. MSCs were first introduced by Friedenstein in 1968 as an element that creates colonies, has fibroblastic phenotype, is adherent and able to regenerate bone tissue *ex vivo* [4]. Further studies proved that MSCs belong to multipotent progenitor cells, able to differentiate into bone, cartilage, and adipose at least. [1]

In 2006, International Society for Cellular Therapy (ISCT) has specified characteristics of a cell to be classified as a MSC. Firstly, it needs to be adherent to plastic during culture. Secondly, a cell needs to express markers CD105, CD73, and CD90 in the absence of hematopoietic antigens such as CD34 and CD45 and other markers typical for lymphocytes B, monocytes, and macrophages. [5] Moreover, MSCs are of a mesodermal germ layer which explains their phenotypic similarity to fibroblasts, their self-renewal ability, and low immunogenicity. Additionally, only one of the two formed cells initiates differentiation process during cell division. [6]

For many years it was thought that the best source of MSCs is bone marrow, possibly because of their initial discovery followed by comprehensive studies. However, bone marrow-derived mesenchymal stem cells (BM-MSCs) are problematic to be obtained since the distressing and unpleasant procedure of bone marrow aspiration narrows down the number of volunteers to donate. Moreover, the amount possible to isolate from each patient is limited and the procedure of biopsy carries the risk to the patient while being under anesthesia. [7] The good alternative to BM-MSCs may be ADSCs.

1.2. Human adipose-derived stem cells

Adipose tissues in mammals distinguish between the white (WAT) and brown (BAT) adipose tissue. WAT supplies tissues with lipids and it acts as energetic fuel or lipid

reconstructive material. BAT, on the other hand, can utilize fatty acids for thermogenesis. Although the role of adipose tissue is crucial for energy homeostasis, its molecular mechanisms are unclear. [8]

The initial role of adipose tissue is to store the energy, insulate body heat and work as mechanical buffer. Adipose tissue consists of mature adipocytes which are surrounded by fibroblasts, nerves, vascular endothelial cells, a variety of immune cells and preadipocytes contained within a stromovascular cell network. Enzymatic digestion of adipose tissue generates a population of adipocyte precursors within a pellet of cells called the stromal vascular fraction (SVF). It comprises in particular of blood cells, endothelial cells, pericytes, adipose precursor cells and multipotent mesenchymal stem cells. [9]

ADSCs have been discovered in 2002 and they are widely studied since then. [10], [11] When compared to BM-MSCs, ADSCs seem to have a lot of advantages. ADSCs belong to the multipotent adult mesenchymal stem cell which is the most promising type when it comes to clinical usage- there is no harvesting difficulties or limited availability like in a case of embryonic stem cells, they do not provoke any ethical issues such as fetal stem cells, and any limitations related to induction procedures while differentiating do not occur just like in a case of pluripotent stem cells. [10] ADSCs can differentiate to mesodermal or trans-mesodermal lineages and give rise to cells that are naturally of ectodermal origin [11].

ADSCs can be harvested through lipoaspiration or abdominoplasty. [12] In addition, ADSCs allow for autologous transplant, which eliminates the requirement of finding a donor, accelerates the process of recovery and provides low invasiveness. Moreover, the fact that adipose tissue consists of huge amounts of stem cells, allows easy access to them.

1.3. ADSCs' phenotype

In recent years great emphasis is placed on a personalized therapy which means that the patient is able to receive targeted treatment. Therefore, not only the therapy is more effective but also the risk of side effects decreases and recovery time shortens. The same applies to stem cell therapy including ADSCs. Thus, obtaining the detailed knowledge about ADSCs phenotype and functionality is crucial to meet the needs of personalized therapy. At the present time the understanding of the above is poor and the improvement is required. By characterizing the ADSCs' phenotypes and assigning the role to each of them this improvement may be reached.

There are many factors affecting the composition of ADSCs. Obtained from SVF stem cells are a heterogeneous population, therefore, the ratio and property may vary along with in vitro expansion. Moreover, differences include not only variations of cells composition but also their regenerative potentials. The location in the body that the adipose tissue comes from is another important aspect. Cells from different body parts differ in their cellular composition with varied phenotype, the quantity and proportion of adipocytes forming it, as well as blood vessel stromal cells and immune system cells among others [13]. Additionally, the stage of isolation and passage makes a difference while comparing the immunophenotype of these populations. The most drastic changes occur in early expansion. [2]

Notably, many different factors generate the phenotype of specific ADSCs populations. Phenotypic characterization of cells allows for identification and quantification

of a specific cell group in the mixed cell population. It may be crucial to determine whether this renders particular therapeutic effects during stem cell therapy. [14], [15]

ASCs have shown to take part in many biological functions of fat tissue, therefore, it is unlikely that only one subset performs in those functions. It was previously proved that some populations are associated with specific functions. For example the presence of $CD166^+$, $CD271^+$, and $CD248^+$ is known for taking part in wound healing process [16]–[18], the existence of $CD200^+$, and $CD274^+$ is associated with immunomodulatory properties [19], [20] and expression of $CD201^+$, $CD36^+$, and Stro-1^+ is reported for its adipogenic differentiation [21]–[23]

If assumed that subsets by expressing specific markers can undergo differentiation specific for the marker, the personalized stem cell combination can be prepared for particular purpose. Consequently, this subset selection maximizes the positive clinical outcome followed by other medical, economical and ethical benefits. [24]

Although ADSCs phenotypic profile is an interesting subject for many researchers, there is still much insight missing. [25], [26] Peng et al. came to the conclusion in their study that further examination of co-expressed surface markers is needed in order to fully understand how the immunophenotypic profile affects the functionality of cell subsets. [2] Focusing on their investigation, this study aims to identify the promising subsets and expand the knowledge of their mechanisms and actions.

1.4. Flow cytometry

Flow cytometry is a commonly used technique by researchers due to its multiple usability. It has the ability to measure and analyze different cells' properties such as its size, shape and complexity of thousands in a matter of minutes. Wild range of applications may be implemented in flow cytometers in particular GFP expression analysis, drug discovery, bacterial viability, DNA analysis, cancer diagnosis and monitoring of HIV/AIDS progression. Three main components of flow cytometry are fluidics, optics, and electronics. [27]

1.4.1. Fluidics

The fluidic part includes the transport of particles from stream to the laser beam for interrogation. The sample flow rate is controlled by adjusting the sample pressure relative to the physiological buffer called sheath fluid (it surrounds the cells) pressure using a pressure regulator. The fluidics system—the tubing, pumps, and valves—organizes the initial sample suspension into a single-file stream of cells as they make their journey through the flow cytometer for analysis. [28]

1.4.2. Optics

The optical system consists of excitation optics and collection optics. The excitation optics (lasers and lenses) allow to focus and shape the laser beam. Thanks to that the beam consistently crosses the interrogation point at a fixed position. Light emitted from the cell is collected by a lens (collection lens) and passed through optical mirrors (dichroic) and filters (bandpass, shortpass, or longpass) which transfers specific wavelengths of light to designated optical detectors. It can be achieved by the collection optics.

Light first travels the laser's path, then is gathered by a collection lens and finally is sent to a diode which converts the light signal into a current. Finally, the signal is recorded by the electronics system. Emitted fluorescence light is collected by a collection lens and rerouted to photomultiplier tubes (PMTs).

Next, a beam is produced by the lasers and focusing lens of light. The beam collides with the cells at the interrogation point. Because of cell interaction with a laser, the light scatter is produced, which is eventually gathered by collection lenses. It is instantly directed to a photodiode or to PMTs. The produced currents are directed to the electronics system. [28]

1.4.3. Electronics

Electronic part function is to convert light signals into electronic signals (voltages) and to perform data analysis. This step can be achieved by either photodiodes, which is usually used to detect strong forward scatter signal, or PMTs, which are able to identify weaker signals. An electronic signal is created when a cell crosses the laser beam and starts to spread light or fluorescence. This light is then converted into electrons by PMTs or photodiode, which are multiplied in order to create a larger current.

The current after being amplified is converted into a voltage pulse. As the cells enter the path of the laser, the voltage pulse increases. Finally, signal processors interpret voltage pulses into numerical values. The cytometer computer receives this for further analysis and storage. [28]

1.4.4. Panel design

The goal while designing the experimental panel is to predict and minimize spectra overlap, to have the highest possible resolution of populations, and to avoid false-positive signals all at the same time. The more biomarkers included in the study, the more complicated the panel design gets. In order to make the panel successful, an in-depth knowledge of the instrument, cell population and fluorochromes is needed.

Since data quality highly depends on a good panel design, it is important to follow the main principles of multicolor layout. First main key point is to place fluorochromes according to their brightness, which means to assign them in agreement with the calculated stain index. [29] Next, is to include all the necessary controls, which will allow for obtaining an accurate data. Equally important is to keep the resolution as high as possible. The resolution, or data spread, decreases along with the higher spillover, therefore, minimizing the potential of spillover is paramount. When it comes to multiple fluorochromes, spreading them across available lasers may be helpful. Lastly, using tandem dyes (e.g. PE-Cy7 or PE-CF594) can be tricky, due to their sensitivity to light and temperature, thus it is crucial to keep them away from exposure to those conditions and degrading eventually. [30]

1.4.5. Controls

In order to make the obtained results significant it is crucial to distinguish the proper data from the background variation. That is why preparing controls for the experiment should be done. There is diverse choice of controls to choose from depending on the desired results. One of them is unstained control (unstained cells) which allows for localization of

the autofluorescence. By using an unstained control it is possible to define negative population as well as cell size, and granularity. [30] Correspondingly, single-stained positive controls (cells stained by each fluorochrome in the panel individually) should be applied. This control allows for setting the compensation. Another one is an isotype control. It consist of antibody raised against an antigen that is not present on the analyzed sample. Although it is considered to be controversial and is not recommended for multicolored experiments, isotype control can be still used as the negative control. [33] Next, fluorescence minus one (FMO) control points out the data-spread caused by high compensation values and is used to localize positive populations. As the name says, FMO control for specific fluorochrome will contain all the fluorochromes from the design minus this specific one. FMO control allows for easy gating of negative population and is recommended for multicolor flow cytometry experiments.

The accuracy and quality of the data are often at risk when the experiment consists of multiple fluorochromes. A detector is able to intercept the fluorescent signal not only from the fluorochrome specific for this detector but also from other fluorochromes present in the design as well as cells' autofluorescence. Wide fluorescence emission peaks may have long tails. Sometimes a peak may overlap and be recognized by different channel because its wavelength filter could read the other fluorochrome signal. This may cause false signal in the detector which is called spillover. In order to reduce spillover signal and correct the measurement of non-primary signal by a detector a compensation is required. [31] For this purpose a wide selection of polystyrene beads, which can be stained for each fluorochrome separately, is provided. Sometimes the only solution is to modify the panel design. While performing compensation the risk of data-spread appears, which may reduce the resolution between populations. Nowadays, computer assisted compensation is a routine. [32]

1.4.6. Antibody titration

Titrating antibodies for flow cytometry purpose is a useful step in effective and economic panel design. It allows to determine which concentration of an antibody leads to saturation as well as assure that the antibody works properly. The required amount is usually lower than the amount recommended by the company. The differences come from the conditions of the experiment which may vary from the conditions of the manufacturer's laboratory, as well as from the time and temperature of the study or cell type. Furthermore, staining with too much of the antibody may lead the fluorescent signal to go off-scale. Thus, the antibody should be titrated and the researcher should not rely on the provided by the manufacturer "Volume per Test". Provided that, the antibody should be tested with the amounts below and above the recommended volume. It is suggested to test 8 to 12 dilutions in order to generate a saturation curve. [34]

1.5. Bioreactor

Bioreactors are widely used as a controlled environment for cell growth and expansion, including MSCs. Its main predominance over culture in a bottle is commercialization. The amount of cells obtained by bioreactor can be consider industrial-scale. Study by Schirmaier et al. proves that more than 3 L volume bioreactors can be used for ADSCs culture. This is a crucial point for clinically relevant studies when huge tissue

grafts are necessary. [35] Even though ADSCs are adherent cells, which not all of the bioreactors are adapted for, the perfusion system of fibers allows for bigger area for cells to be attached. Another important factor is the reproducibility which is much higher compared to regular flask cultures. This is critical when implementing therapy in the clinic. [36]

2. Methods

The workflow of the experiment was shown in Figure 2. All the protocols used during the study belong to the Regenerative Medicine Group from Department of Health Science and Technology, Aalborg University. The fat tissue was kindly donated by Aleris-Hamlet Private Hospital, Aalborg. The isolated stem cells were used to conduct flow cytometry analysis at P1, P4, and P8.

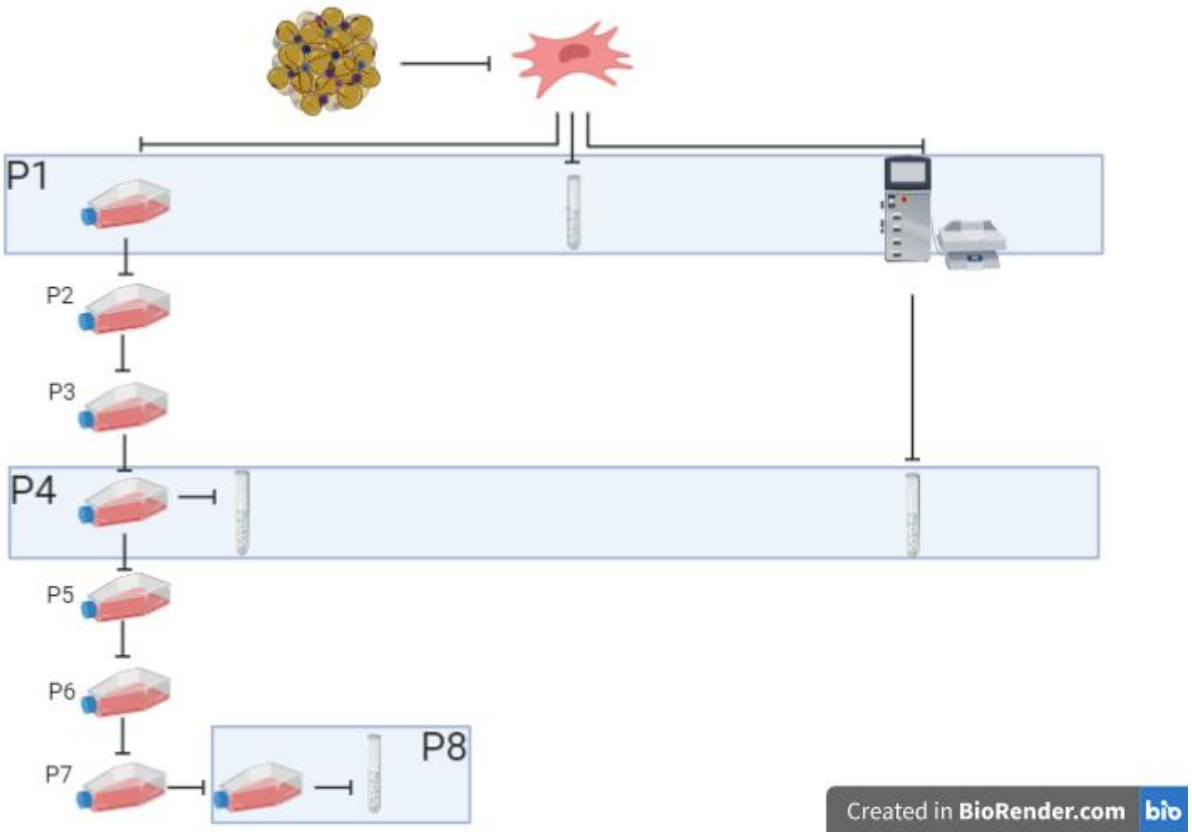

Figure 2. The workflow of the experiment. The obtained SVF was divided- ⅕ of cells was seeded in T175 bottle for culturing and ⅘ was placed in the bioreactor. When the cells in the bottle have reached the confluency of 80-90% they were passaged until P8. The flow cytometry was performed for cells from P1, P4, and P8 respectively as well as for the cells from bioreactor.

2.1. Flow cytometry

2.1.1. Marker selection and panel design

13 markers have been chosen to be a part of a panel design for this experiment, 8 of which were primarily known as weakly expressed in ACSs (CD36, CD34, CD248, CD200, CD271, CD274, CD146, Stro-1), and 5 of which were primarily known as strongly expressed by ADSCs (CD201, CD73, CD90, CD105, CD166). Each one of them was selected due to previously reported nomenclature focusing on their properties and application associated with ADSCs which was summarized in Table 1.

Table 1. The list of markers of interest and their properties. The list includes strongly expressed markers and weakly expressed markers chosen to be part of a panel design in this experiment.

Marker	***Properties/ Application***
CD36	obtains adipogenic and triglyceride accumulation potential; CD36 is also known for facilitating lipid uptake in immature adipocytes progenitors [21]
CD34	plays important role in fat graft healing and its concentration may be used to predict the graft retention [37]; several studies indicate CD34 expression loss during *in vitro* culture [38]; CD34+/CD271+ subsets are known to be able to undergo osteogenic differentiation; [39]
CD248	its positive expression is associated with proinflammatory and profibrotic pathways; arbitrates part of the adipose tissue response to hypoxia as a microenvironmental sensor; [16]
CD200	also known as OX2; associated with adipogenic capacities; related to the expression of CD10- visceral adipose-derived ADSCs have higher expression of CD200, whereas subcutaneous ADSCs express higher levels of CD10; [19]
CD271	increases cartilage repair and bone formation; takes part in adipogenic differentiation; has impact in wound healing; $CD271^+$ MSCs have low angiogenic activity and they improve tissue repair [17]; associated with multipotency [40]; its expression may decrease after culture expansion [41];
CD274	also known as PD-L1 (programmed death ligand 1); cell surface marker of adipose tissue; comprise immunomodulatory properties; [20], [42]
CD146	also called cell surface glycoprotein MUC18 [43]; takes part in wound healing; adipose-derived CD146+ pericytes display complementary roles in bone healing [44]; proven to regulate tissue development and its homeostasis [45]; has adipogenic potential [46];
Stro-1	determines cells multi-lineage potential; takes part in osteogenic differentiation; [23], [47] its expression in adipose tissue was determined in the endothelium of arterioles, capillaries, and some adipose tissue veins [48]; generally lower expression in ADSCs than in BMSCs [49];
CD201	cell surface marker also called endothelial protein C receptor; promotes adipogenic differentiation both *in vivo* and *in vitro*; [22], [50] yields much higher expression in ADSCs than in BMSCs [51];
CD73	takes part in adipogenic and osteogenic differentiation; has higher capacity for cardiomyocytes differentiation *in vitro*; characterized by high inconsistency expression in different subpopulations; [52]
CD90	also called Thy-1; engaged in adipogenic differentiation as well as adipose tissue homeostasis and metabolism; [53] CD34+/CD90+ ADSCs have capability to differentiate into endothelial cells as well as they can form capillary-like structures [26]; has high capacity of forming chondroblasts and osteoblasts; takes part in allowing cells to become immortal and multipotent; [54]
CD105	is able to distinguish adherent ADSCs from hematopoietic lineages [55]; takes part in allowing cells to become immortal and multipotent [54]; holds osteoblastic and chondroblastic potency; decreased expression of $CD105^+$ is proven to increase osteogenesis; [55]
CD166	also called activated lymphocyte cell adhesion molecule (ALCAM) [56]; takes part in wound healing and osteogenic differentiation [18];

The markers of choice depicted in Table 1. were divided into two panels, according to its previous expression described in nomenclature, low spill over rate as well as the amount and localization of bandpass filters in the flow cytometer. The final view of the panel designs was shown in Table 2. and Table 3.

Table 2. Panel 1. The list of lasers and filters available in the experiment together with the arrangement of the weakly expressed markers. The table includes the names of the markers as well as their dyes layout.

Weakly expressed markers- Panel design				
Laser	**Filter**	**Dye**	**Marker**	**Company Cat. number**
355 nm	395/25	BUV395	CD36	BD Biosciences 565422
	525/50	BUV496	CD34	BD Biosciences 749903
	740/40	BUV737	CD248	BD Biosciences 748753
488 nm	513/26	BB515	CD200	BD Biosciences 564580
	576/21			
	620/29			
	671/30			
	710/45	BB700	CD271	BD Biosciences 746140
	795/70			
561 nm	579/16		fvs570	BD Biosciences 564995
	614/20	PE-CF594	CD274	BD Biosciences 563742
	785/60	PE-Cy7	CD146	BD Biosciences 562135
640 nm	664/22	APC	Stro-1	Invitrogen 534086
	692/75			
	795/70			

Table 3. Panel 2. The list of lasers and filters available in the experiment together with the arrangement of the strongly expressed markers. The table includes the names of the markers as well as their dyes layout.

Strongly expressed markers- Panel design				
Laser	**Filter**	**Dye**	**Marker**	**Company Cat. number**
355 nm	395/25	BUV395	CD201	BD Biosciences 743557
	525/50			
	740/40			
488 nm	513/26	FITC	CD73	BD Biosciences 561254
	576/21			
	620/29			
	671/30			
	710/45	PerCP-Cy5.5	CD90	BD Biosciences 561557
	795/70			
561 nm	579/16		fvs570	BD Biosciences 564995
	614/20	PE-CF594	CD105	BD Biosciences 562380
	785/60			
640 nm	664/22	AlexaFluor®647	CD166	BD Biosciences 564938
	692/75			
	795/70			

2.1.2. Experiment setup and cell staining

2.1.2.1. Dead cells percentage

Before antibody staining, the cells were stained with Fixable Viability Stain 570 (FVS570) (BD Biosciences) in order to tell apart the dead and alive cells during flow cytometry. In order to do that the cell suspension was centrifuged (300g, 5 min) and then resuspended with PBS with the addition of FVS570. After incubating for 15 min in room temperature, the cells have been washed again and centrifuged. Finally, the pellet has been resuspended in fetal bovine serum (FBS, Gibco) and distributed into Eppendorf tubes. The cells remained covered and were kept on ice.

2.1.2.2. Controls

Antibody mixes were prepared according to the procedure description in the Appendix 1. with the implementation of FMO control. Despite that, the unstained cells sample was prepared in order to determine the localization of the negative population. The panel with weakly expressed markers consisted of two or more BD Horizon Brilliant dyes, which prompted the usage of BD Horizon Brilliant Stain Buffer (BD Biosciences) as a diluent. For the panel with strongly expressed markers, FBS was used for the same purpose. In the meantime Eppendorf tubes with cell suspension were centrifuged (300g, 5 min) and the supernatant was discarded. Prior to the addition of the antibody mixtures, they were placed on Vortex and mixed thoroughly, and then added to the cell pellet respectively. Henceforth, the stained cells were incubated in a cooled room on a Belly Dancer orbital shaker for 30 min covered in tinfoil. When the incubation was over, the cells were washed twice with FBS due to cell aggregation risk. Lastly, they were resuspended in FBS and placed in polystyrene FACS Tubes.

Quality control (QC) was implemented daily by the use of SPHEROTM Ultra Rainbow Fluorescent Particles (3.0 μm., 2ml, Nordic BioSite) in order to ensure accurate results.

Compensation values were established with the usage of CompBeads Plus Set Anti-mouse Ig, κ, and CompBeads Plus Set Anti-rat Ig, κ (both from BD Biosciences). The compensation matrix was created based on the dot-plots outlines visible on each channel used in this experiment.

2.2. Isolation of ADSCs

Lipoaspirate was washed thoroughly with phosphate-buffered saline (PBS; Gibco, Taastrup, Denmark) in order to remove vascular residues and blood cells. When washed, PBS was removed and lipoaspirate was divided into 50 ml centrifuge tubes up to half of the volume. Then, the collagenase buffer was prepared by dissolving Collagenase NB 4 Standard Grade from *Clostridium histolyticum* (0,12 U/mg => 0,6 U/ml) (Nordmark Biochemicals, Uetersen, Germany) in a Hanks balanced salt solution (10x HBSS, Gibco) and filtering it through a 0,22 μm filter before use. The collagenase was used in order to cleave the peptide bonds in the triple helical collagen. The obtained compound was added in a remained volume to lipoaspirate and was incubated under continuous agitation at 37°C for 45-60 min. Further, the mixture was filtered through 100 μm filter (Millipore, Omaha, NE) with the use of vacuum and then centrifuged at 400g for 10 min. After discarding the supernatant, the pellet was resuspended in Alpha-Minimum Essential Medium (1X) +

GlutaMAX™ (supplemented with 10% fetal calf serum (FCS) and 1% antibiotics) (all from Gibco) and filtered again through a 60 μm filter (Millipore). Finally, the solution was centrifuged at 400g for 10 min. The collected pellet was resuspended in the growth medium. Lastly, by the use of the Nucleocounter NC-200 cell counter (Chemometec, Allerod, Denmark) the cell yield was determined.

2.3. Bioreactor

The instrument used in this experiment is The Quantum® Cell Expansion System (TerumoBCT). A fresh Alpha-Minimum Essential Medium (1X) supplemented with GlutaMAXTM (supplemented with 10% fetal calf serum [FCS] and 1% antibiotics) (all from Gibco) bag was prepared for cell loading and attached to the expansion set. Coating reagents were passed through a filter prior to integrating with cells. The concentration of lactic acid and glucose was measured as a control. The cell inlet bag was inserted in the System and the additional air was removed. The uniform cell suspension program was chosen.

2.4. Cell culture

The acquired cells were seeded into T175 culture bottles (Greiner Bio-one, Frickenhausen, Germany) and were passaged until passage 8 (P8). The required density in each bottle was 5000 cells/cm2. Every passage was implemented when the cells reached confluency of 80-90%. The cells were firstly detached from the bottom of the bottle by TryPLE (Gibco) and secondly washed in PBS before transferring to the new bottle. Prior to this, the medium was changed every 2-3 days until the confluency has been reached.

The cells that reached confluency at P1, P4 and P8 have been prepared to be examined by the flow cytometry. First step was to wash the cells twice with PBS. Next the cells were detached from plastic by adding TryPLE (Gibco) followed by short incubation in 37°C. Next, the bottle was washed thoroughly with PBS (1:3) to make sure no cells stay adherent to the wall as well as to inactivate the TryPLE function. The suspension was centrifuged at 300g for 5 min and the supernatant was discarded. After resuspending the pellet in PBS the cell yield needed to be determined. ⅓ of the cells was seeded freshly in the new T175 bottle for next passages and the remaining cells were forwarded to flow cytometry procedure.

2.5. Data analysis

The data was analyzed in the Kaluza 2.1 software package (Beckman Coulter). The graphs were prepared in GraphPad Prism.

3. Results

3.1. Morphology of the cells

The fraction isolated from fat tissue was seeded in the flask. Control pictures were taken in P1, P2, and P3 (Figure 3). Between P1 and P2 the most dramatic changes occur. Fat droplets and cell clumps displayed in P1 disappear in P2. Cell shape changes in P2 into fibroblast-like elongated shape. Changes taking place in P2 remain along the later passages.

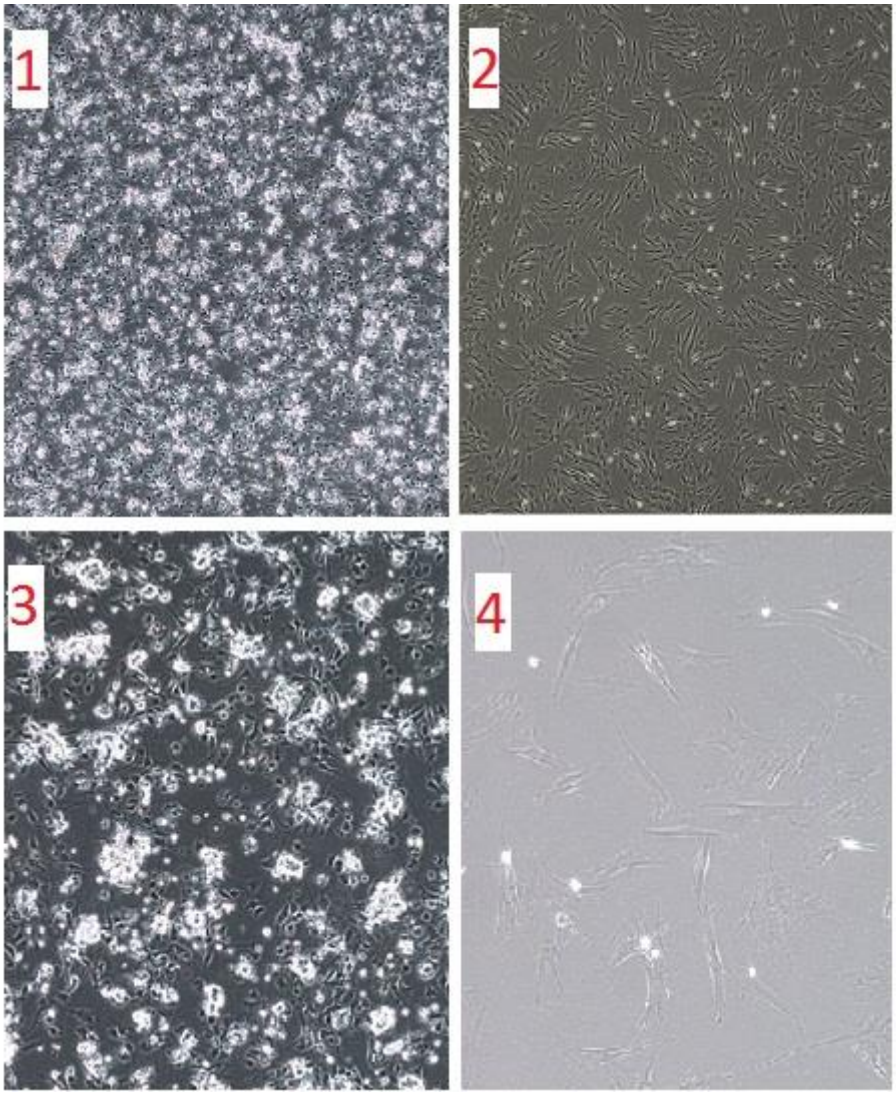

Figure 3. The view of the cells in P1 and P2. The legend: 1- P1, day 1, magnification 40; 2- P2, day 1, magnification 40; 3- P1, day 1, magnification 100; 4- P2, day 1, magnification 100

3.2. Gating process

In order to remove all the noise, debris, dead cells, unstable flow and droplets, the gating strategy was implemented. By establishing gates, the data accuracy improves and the analysis becomes easily reproducible.

First step was to gate the positive cell population and separate it from the debris (Figure 4). This process removes autofluorescence and background staining from the actual cell population. Next, thanks to implementing the viability staining (FVS570), the gate for

alive cells was created with the input gate of positive cell population (Figure 5.). This process allows for removing dead cells, or cells in the process of dying from the analysis.

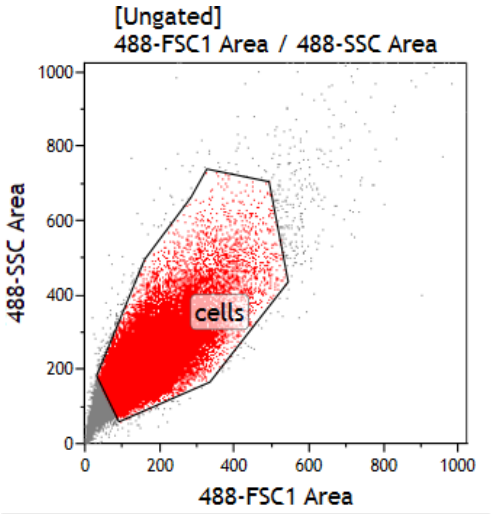

Gate	Number	%Total	%Gated
All	158,327	100.00	100.00
cells	140,480	88.73	88.73

Figure 4. Gating process of positive populations. The dot plot displays the gating process of positive cells out of all of the cells present in the sample. Below the dot plot the number of gated cells and the percentage is shown. The gate used in this process is polygon. Example: P4, Panel 1

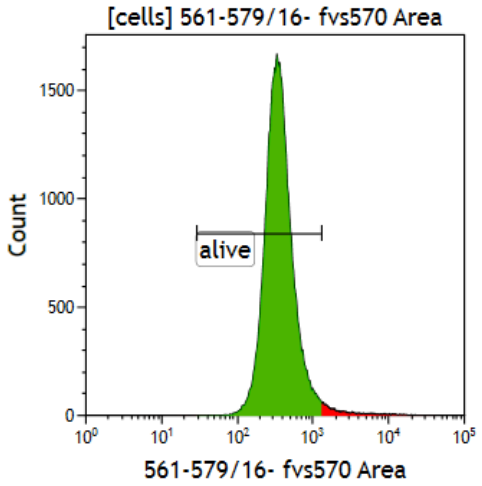

Gate	Number	%Total	%Gated
All	140,480	88.73	100.00
alive	136,245	86.05	96.99

Figure 5. Gating process of alive cells. All histograms display the gating process of alive cells out of the gated positive cells (Figure 3.). Below histogram the number of gated cells and the percentage is shown. The gate used in this process is linear. Example: P4, Panel 1

Next, the ‘singles’ gate was created. In the interrogation point only one, single cell can be analyzed. Therefore, it is crucial to eliminate clumps of cells or cells that were located too close from each other that the laser could not separate them (coincident event). The gate was established along the diagonal in a dot plot FSC Area/ FSC Height were single cells are located (Figure 6).

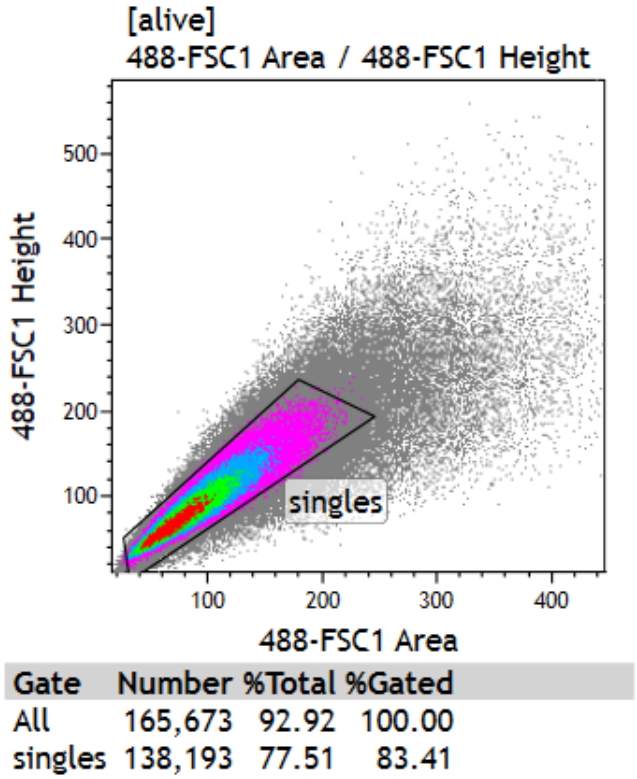

Gate	Number	%Total	%Gated
All	165,673	92.92	100.00
singles	138,193	77.51	83.41

Figure 6. Gating process of 'singles'. The dot plot displays the gating process of single cells. Below the dot plot the number of gated cells and the percentage is shown. The gate used in this process is polygon. Example: P4, Panel 1

It is necessary to assure the stream of the tested cells was not interrupted by clogged cells present in the suction tube, or that the data was not affected by back pressure. In order to do that the time plot with the stability flow gate was established with the input gate of alive cells (Figure 7.).

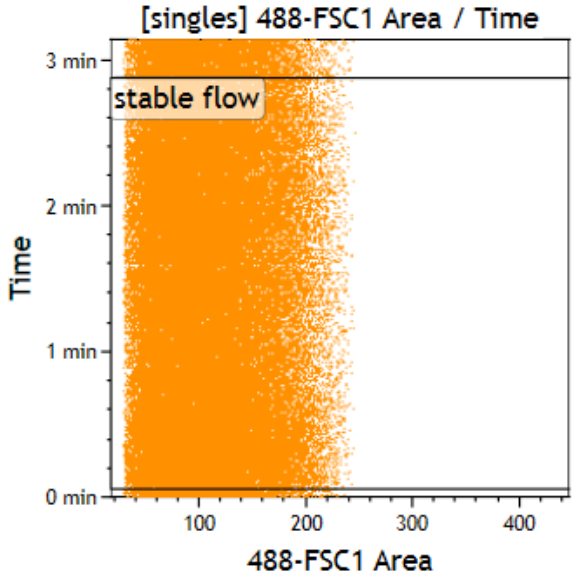

Gate	Number	%Total	%Gated
All	138,193	77.51	100.00
stable flow	125,782	70.54	91.02

Figure 7. Gating process of stable flow. Dot plot displays the gating process of stable flow out of the gated 'singles' cells (Figure 6.). Below dot plot the number of gated cells and the percentage is shown. The gate used in this process is rectangle.

Finally, the step to evaluate the expression of each marker is needed. Overlay histogram shows how the FMO controls are used to assess the expression of a specific marker (Figure 8). The gate were established around 2,5% of FMO peaks for each marker.

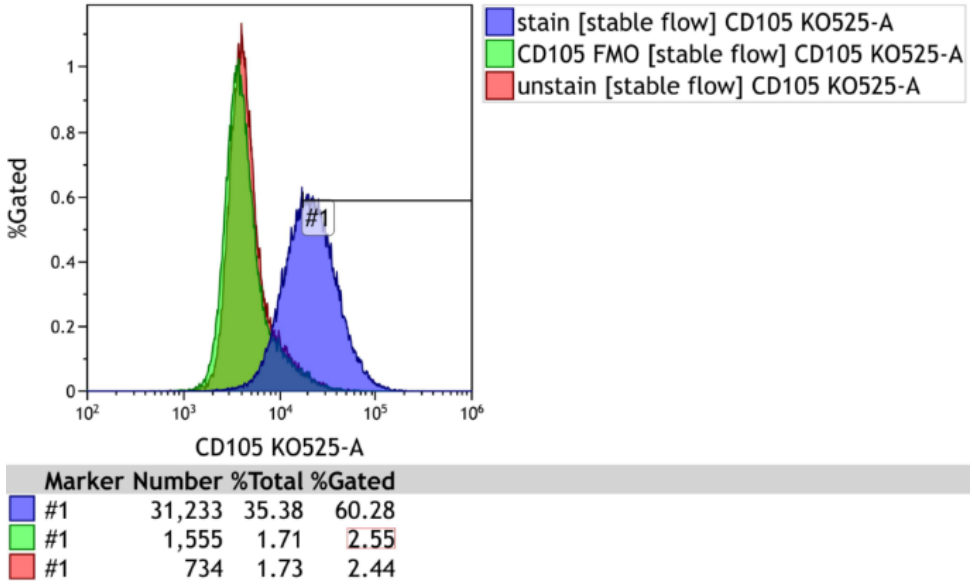

Figure 8. Overlay of FMO control, unstained sample and stained sample peaks. Histogram displays the overlay of peaks which shows how the FMO controls allows for localization of the marker. Example: CD105 at P4

3.3. Population percentage in P1, P4 and P8

Even though the experiment tested 13 markers in two panels not many possible combinations were found with the significant expression. In Panel 1 (weakly expressed markers) subset CD146-CD200-CD248-CD271-CD274+CD34-CD36-Stro-1- was found to highly express tested markers in P1, P4, and P8, and subset CD146+CD200-CD248-CD271-CD274+CD34-CD36-Stro-1- was found to highly express tested markers in P4, and P8 (Table 4.). In Panel 2 (strongly expressed markers) combination CD105+CD166+CD201+CD73+CD90+ was highly expressed in P1, P4, and P8, and subset CD105+CD16+-CD201-CD73+CD90+ was highly expressed in P4 and P8 (Table 5). The diversity of these highly expressive populations was presented in Figure 9.

Table 4. Population percentage of P1, P4 and P8 in Panel 1. Only populations with the expression higher than 5% were included in this table. The percentage of each population in specific passage was obtained by creating a tree of all stained markers. The tree view example is displayed in Appendix 2.

Panel 1

Population	P1	P4	P8
CD146-CD200-CD248-CD271-CD274-CD34-CD36-Stro-1-	17,74%	0%	0%
CD146+CD200-CD248-CD271-CD274+CD34-CD36-Stro-1-	0%	39,40%	56,58%
CD146-CD200-CD248-CD271-CD274+CD34-CD36-Stro-1-	9,01%	38,42%	19,48%
CD146+CD200-CD248-CD271-CD274+CD34-CD36+Stro-1-	0%	0%	6,88%
CD146-CD200-CD248-CD271-CD274-CD34+CD36-Stro-1-	12,20%	0%	0%
CD146-CD200-CD248-CD271-CD274-CD34-CD36-Stro-1-	17,74%	0%	0%
CD146-CD200-CD248-CD271-CD274+CD34+CD36-Stro-1-	11,46%	0%	0%
CD146+CD200-CD248-CD271-CD274-CD34-CD36-Stro-1-	5,63%	0%	0%
CD146+CD200-CD248-CD271-CD274-CD34+CD36-Stro-1-	5,49%	0%	0%
CD146+CD200-CD248-CD271-CD274+CD34+CD36-Stro-1-	6,70%	0%	0%

Table 5. Population percentage of P1, P4 and P8 in Panel 2. Only populations with the expression higher than 5% were included in this table. The percentage of each population in specific passage was obtained by creating a tree of all stained markers. The tree view example is displayed in Appendix 2.

Panel 2

Population	P1	P4	P8
CD105+CD166+CD201+CD73+CD90+	71,48%	86,56%	82,62%
CD105+CD166+CD201-CD73+CD90+	3,71%	11,80%	16,07%
CD105+CD166-CD201+CD73+CD90+	9,85%	0%	0%

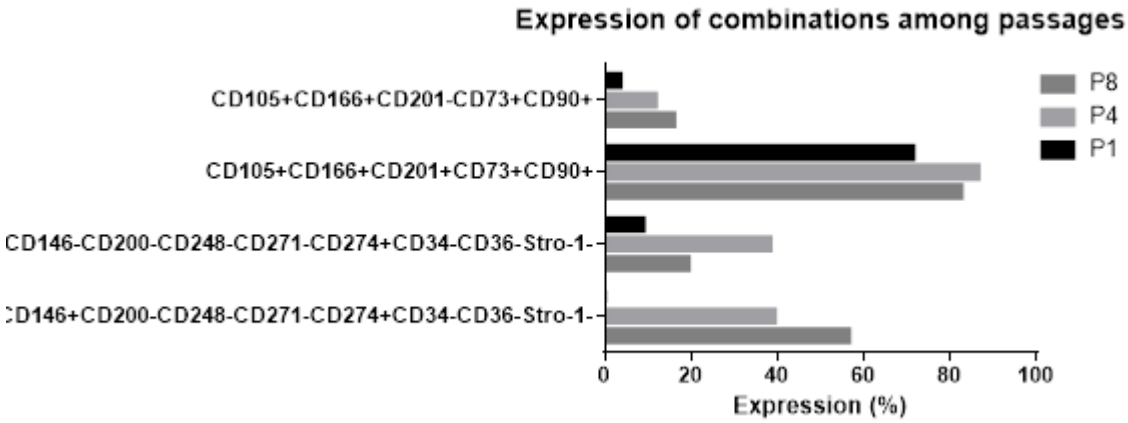

Figure 9. Expression of combinations upon passages. Each expression of a specific subset was depicted upon three passages- P1, P4, and P8. The chart was created in GraphPad Prism.

3.4. Comparison of bioreactor cultured populations and regular flask cultures (P4)

In Panel 1 none of the subsets retrieved from bioreactor was comparable to P4 from flask (Table 6.). In Panel 2, two compositions with the expression higher than 5% were adequate to the compositions expressed in P4 (Table 7.).

Table 6. Comparison of bioreactor cultured populations and regular flask cultures (P4) in Panel 1. The percentage of populations obtained from bioreactor and from flask (P4) was retrieved by creating a tree of all stained markers. The tree view example is displayed in Appendix 2. The table contains only populations with expression higher than 5%.

Panel 1

Population	Bioreactor	P4 (flask)
CD146-CD200+CD248-CD271+CD274-CD34-CD36-Stro-1-	49,31%	0%
CD146+CD200+CD248-CD271+CD274-CD34-CD36-Stro-1-	17,89%	0%
CD146-CD200+CD248+CD271+CD274-CD34-CD36-Stro-1-	8,16%	0%

Table 7. Comparison of bioreactor cultured populations and regular flask cultures (P4) in Panel 2. The percentage of populations obtained from bioreactor and from flask (P4) was retrieved by creating a tree of all stained markers. The tree view example is displayed in Appendix 2. The table contains only populations with expression higher than 5%.

Panel 2

Population	Bioreactor	P4 (flask)
CD105+CD166+CD201+CD73+CD90+	33,80%	86,56%
CD105+CD166+CD201-CD73+CD90+	61,39%	11,80%

3.5. Viability

The cells viability was consistent upon different passages and after culturing in bioreactor (Figure 10).

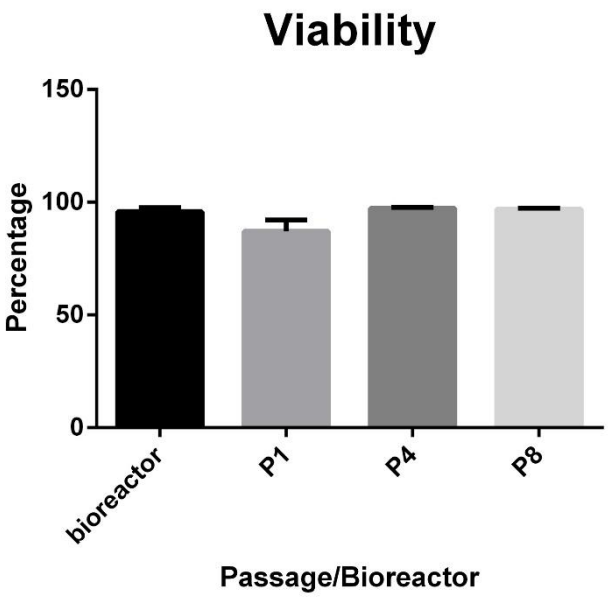

Figure 10. Changes of cells viability throughout the passages (P1, P4, and P8) and bioreactor. Standard deviation (SD) and the chart were created in GraphPad Prism. SD value: bioreactor (1,76), P1 (4,96), P4 (0,38), P8 (0,44).

4. Discussion

4.1. Subsets expression

This study was able to identify four combinations of co-expressed markers with the expression higher than 5%, two of which are 5-marker combinations, and two are 8-marker combinations. The most promising phenotype seems to be CD105+CD166+CD200-CD73+CD90+ since the expression trend was rising. Throughout the cell culture dynamic expression changes occurred, which ADSCs are commonly characterized by [57]. Despite that, mentioned subsets were capable of keeping their expression stable upon passages. This stability encourages further research.

Prior to the study, the consistent high expression of markers CD90, CD105, and CD73 was already expected as they are known MSCs markers. They tend to characterize cells in early stage of differentiation, therefore, their presence in the subset may be beneficial for widespread differentiation in the tissue. [24]

None of the identified combinations expressed marker CD34 which is contradictory to the research by Philips et al. [37]. Their study not only declares high expression of this marker among different SVF donors but also correlates its expression to fat graft retention. In this experiment expression of CD34 was featured in P1 but its expression decreased in next passages. This is supported by Bear et al. who stated that the expression of CD34 may present in the early stage of culture and be lost after a passage. [57] This may be due to environmental conditions which cells are not familiar with and are not able to adapt to.

Marker CD274 primarily known to be weakly expressed, have shown significant expression throughout the passages. This finding, when investigated further, may be a valuable outcome for immuno- and cancer therapy, as CD274 is currently in clinical use but with the need of being stimulated by interferon gamma. [58]

Markers Stro-1 and CD36 have shown consistent low expression in all passages with the expression below 5%. Therefore, cell stimulation may be required if the need of their further investigation occurs.

Cell number was inconsistent throughout the passages, with the amount of 20.289 (51,28%), 140.480 (88,73%), and 79.291 (32,63%) respectively. However, the gating process is human-dependent, and mostly depends on visual examination of the dot plots, therefore, such diversity is possible and unlikely affects other results.

4.2. Principle of bioreactor

Implementing of bioreactor grown culture was introduced in order to examine ADSCs' expansion in stable, large-scale conditions. Study measuring MSCs doubling time proved bioreactor to be able to harvest more cells than flask culture.[59] Results obtained from bioreactor were compared to results obtained from P4. More cells were obtained from flask culture which is contradictory to study by Frank et al.[59] The reason may be connected to the differences in the protocol's settings in both studies.

There was no common subsets identified between populations harvested from bioreactor and from the flask in Panel 1. Although, there are two commonly expressed subsets in Panel 2. This founding, even though needs more investigation, allows for questioning whether stable conditions present in bioreactor are more ADSCs specific than

flask culture. Usage of bioreactor would be beneficial for clinical utility as more quantity of cells can be harvested and the conditions are automatically stabilized but more research is required.

4.3. Future perspectives

Due to unforeseen circumstances unrelated to the study design, the experiment was conducted on one SVF donor only. In order to make the results more significant the number of donors should be expanded. After that it would be clear which subpopulations are distinct and can undergo the fluorescence-activated sorting process. Given that different subpopulations may be applied for various purposes, it is essential to explore their biological properties. Thus, functional tests such as immunoregulatory profile testing, and transcriptomic profiling by scRNA-seq are highly relevant for further investigation. If the results of some single clonal populations occur significant for being implemented in regenerative medicine (e.g. wound healing), an animal trial can be conducted.

5. Conclusion

Adipose tissue is a great source of large quantities of stem cells which can be obtained in a pain- and risk free process of lipoaspiration. Moreover, the patient may be a graft donor at the same time. Despite current clinical use of ADSCs, the knowledge about their subsets as well as the role is limited and requires detailed investigation. This study focused on identification of ADSCs subsets by the use of multicolor flow cytometry. Five subsets in total have shown high expression but only three remained highly expressed after P1. Moreover, the study implemented a innovative technique of culturing adherent cells in bioreactor and compared the cell yield and viability to cells cultured in flask. Unfortunately, no significant benefits, besides keeping the culturing conditions stable, were observed. All things considered, further investigation is required in order to match the obtained subsets' phenotypes with their functionality.

References

[1] A. Trounson and C. McDonald, "Stem Cell Therapies in Clinical Trials: Progress and Challenges," *Cell Stem Cell*, vol. 17, no. 1, pp. 11–22, 2015, doi: 10.1016/j.stem.2015.06.007.

[2] Q. Peng, H. Alipour, S. Porsborg, T. Fink, and V. Zachar, "Evolution of asc immunophenotypical subsets during expansion in vitro," *Int. J. Mol. Sci.*, vol. 21, no. 4, 2020, doi: 10.3390/ijms21041408.

[3] A. A. Dayem *et al.*, "Production of mesenchymal stem cells through stem cell reprogramming," *Int. J. Mol. Sci.*, vol. 20, no. 8, pp. 1–42, 2019, doi: 10.3390/ijms20081922.

[4] G. P. F. A J Friedenstein, K V Petrakova, A I Kurolesova, *Heterotopic of Bone Marrow. Analysis of Precursor Cells for Osteogenic and Hematopoietic Tissues*. 1968.

[5] M. Dominici *et al.*, "Minimal criteria for defining multipotent mesenchymal stromal cells. The International Society for Cellular Therapy position statement," *Cytotherapy*, vol. 8, no. 4, pp. 315–317, 2006, doi: 10.1080/14653240600855905.

[6] M. F. Pittenger *et al.*, "Multilineage potential of adult human mesenchymal stem cells," *Science (80-.).*, vol. 284, no. 5411, pp. 143–147, 1999, doi: 10.1126/science.284.5411.143.

[7] M. Strioga, S. Viswanathan, A. Darinskas, O. Slaby, and J. Michalek, "Same or not the same? comparison of adipose tissue-derived versus bone marrow-derived mesenchymal stem and stromal cells," *Stem Cells Dev.*, vol. 21, no. 14, pp. 2724–2752, 2012, doi: 10.1089/scd.2011.0722.

[8] Y. H. Lee, E. P. Mottillo, and J. G. Granneman, "Adipose tissue plasticity from WAT to BAT and in between," *Biochim. Biophys. Acta - Mol. Basis Dis.*, vol. 1842, no. 3, pp. 358–369, 2014, doi: 10.1016/j.bbadis.2013.05.011.

[9] J. Buyse and E. Decuypere, "Adipose Tissue and Lipid Metabolism," *Sturkie's Avian Physiol. Sixth Ed.*, pp. 443–453, 2015, doi: 10.1016/B978-0-12-407160-5.00019-1.

[10] V. V. Miana and E. A. Prieto González, "Adipose tissue stem cells in regenerative medicine," *Ecancermedicalscience*, vol. 12, pp. 1–14, 2018, doi: 10.3332/ecancer.2018.822.

[11] P. A. Zuk *et al.*, "Multilineage cells from human adipose tissue: Implications for cell-based therapies," *Tissue Eng.*, vol. 7, no. 2, pp. 211–228, 2001, doi: 10.1089/107632701300062859.

[12] J. C. Brown, H. Shang, Y. Li, N. Yang, N. Patel, and A. J. Katz, "Isolation of Adipose-Derived Stromal Vascular Fraction Cells Using a Novel Point-of-Care Device: Cell Characterization and Review of the Literature," *Tissue Eng. - Part C Methods*, vol. 23, no. 3, pp. 125–135, 2017, doi: 10.1089/ten.tec.2016.0377.

[13] M. Coelho, T. Oliveira, and R. Fernandes, "Biochemistry of adipose tissue: An endocrine organ," *Arch. Med. Sci.*, vol. 9, no. 2, pp. 191–200, 2013, doi: 10.5114/aoms.2013.33181.

[14] J. B. Mitchell *et al.*, "Immunophenotype of Human Adipose-Derived Cells: Temporal Changes in Stromal-Associated and Stem Cell-Associated Markers," *Stem Cells*, vol. 24, no. 2, pp. 376–385, 2006, doi: 10.1634/stemcells.2005-0234.

[15] F. M. Nielsen *et al.*, "Discrete adipose-derived stem cell subpopulations may display

differential functionality after in vitro expansion despite convergence to a common phenotype distribution," *Stem Cell Res. Ther.*, vol. 7, no. 1, pp. 1–13, 2016, doi: 10.1186/s13287-016-0435-8.

[16] P. Petrus *et al.*, "Specific loss of adipocyte CD248 improves metabolic health via reduced white adipose tissue hypoxia, fibrosis and inflammation," *EBioMedicine*, vol. 44, pp. 489–501, 2019, doi: 10.1016/j.ebiom.2019.05.057.

[17] N. Kohli *et al.*, "CD271-selected mesenchymal stem cells from adipose tissue enhance cartilage repair and are less angiogenic than plastic adherent mesenchymal stem cells," *Sci. Rep.*, vol. 9, no. 1, pp. 1–12, 2019, doi: 10.1038/s41598-019-39715-z.

[18] Z. Mohammadi *et al.*, "Differentiation of adipocytes and osteocytes from human adipose and placental mesenchymal stem cells," *Iran. J. Basic Med. Sci.*, vol. 18, no. 3, pp. 259–266, 2015, doi: 10.22038/ijbms.2015.4129.

[19] W. K. Ong *et al.*, "Identification of specific cell-surface markers of adipose-derived stem cells from subcutaneous and visceral fat depots," *Stem Cell Reports*, vol. 2, no. 2, pp. 171–179, 2014, doi: 10.1016/j.stemcr.2014.01.002.

[20] R. N. Bárcia *et al.*, "What makes umbilical cord tissue-derived mesenchymal stromal cells superior immunomodulators when compared to bone marrow derived mesenchymal stromal cells?," *Stem Cells Int.*, vol. 2015, 2015, doi: 10.1155/2015/583984.

[21] H. Gao *et al.*, "CD36 Is a Marker of Human Adipocyte Progenitors with Pronounced Adipogenic and Triglyceride Accumulation Potential," *Stem Cells*, vol. 35, no. 7, pp. 1799–1814, 2017, doi: 10.1002/stem.2635.

[22] A. Uezumi *et al.*, "Cell-Surface Protein Profiling Identifies Distinctive Markers of Progenitor Cells in Human Skeletal Muscle," *Stem Cell Reports*, vol. 7, no. 2, pp. 263–278, 2016, doi: 10.1016/j.stemcr.2016.07.004.

[23] J. E. Dennis, J. P. Carbillet, A. I. Caplan, and P. Charbord, "The STRO-1+ marrow cell population is multipotential," *Cells Tissues Organs*, vol. 170, no. 2–3, pp. 73–82, 2001, doi: 10.1159/000046182.

[24] K. S. Johal, V. C. Lees, and A. J. Reid, "Adipose-derived stem cells: Selecting for translational success," *Regen. Med.*, vol. 10, no. 1, pp. 79–96, 2015, doi: 10.2217/rme.14.72.

[25] F. De Francesco *et al.*, "Human CD34+/CD90+ ASCs are capable of growing as sphere clusters, producing high levels of VEGF and forming capillaries," *PLoS One*, vol. 4, no. 8, pp. 1–13, 2009, doi: 10.1371/journal.pone.0006537.

[26] M. F. Pittenger *et al.*, "Human adipose CD34+CD90+ stem cells and collagen scaffold constructs grafted in vivo fabricate loose connective and adipose tissues," *Stem Cells Dev.*, vol. 7, no. 1, pp. 1–13, 2013, doi: 10.1016/j.stemcr.2016.07.004.

[27] A. Cossarizza *et al.*, "Guidelines for the use of flow cytometry and cell sorting in immunological studies," *Eur. J. Immunol.*, vol. 47, no. 10, pp. 1584–1797, 2017, doi: 10.1002/eji.201646632.

[28] K. M. McKinnon, "Flow cytometry: An overview," *Curr. Protoc. Immunol.*, vol. 2018, pp. 5.1.1-5.1.11, 2018, doi: 10.1002/cpim.40.

[29] Abcam, “Multicolor flow cytometry panel design,” p. 32.

[30] BD Biosciences, “Principles of Panel Design.” https://www.bdbiosciences.com/documents/BD_Webinar-MulticolorFlowCytometry_01_09.pdf.

[31] J. A. DiGiuseppe and J. Cardinali, “Improved compensation of the fluorochrome AmCyan using cellular controls,” *Cytom. Part B - Clin. Cytom.*, vol. 80 B, no. 3, pp. 191–194, 2011, doi: 10.1002/cyto.b.20584.

[32] A. Adan, G. Alizada, Y. Kiraz, Y. Baran, and A. Nalbant, “Flow cytometry: basic principles and applications,” *Crit. Rev. Biotechnol.*, vol. 37, no. 2, pp. 163–176, 2017, doi: 10.3109/07388551.2015.1128876.

[33] T. P. Bushnell, “When To Use (And Not Use) Flow Cytometry Isotype Controls.” https://expert.cheekyscientist.com/when-to-use-and-not-use-flow-cytometry-isotype-controls/.

[34] M. Kantor, A. and Roederer, “FACS analysis of lymphocytes.,” in *Handbook of Experimental Immunology*, Fifth., Cambridge, 1997, pp. 49.1-.130.

[35] C. Schirmaier *et al.*, “Scale-up of adipose tissue-derived mesenchymal stem cell production in stirred single-use bioreactors under low-serum conditions,” *Eng. Life Sci.*, vol. 14, no. 3, pp. 292–303, 2014, doi: 10.1002/elsc.201300134.

[36] W. Grayson and M. Stephenson, “Recent advances in bioreactors for cell-based therapies [version 1; referees: 2 approved],” *F1000Research*, vol. 7, no. 0, pp. 1–9, 2018, doi: 10.12688/f1000research.12533.1.

[37] B. J. Philips *et al.*, “Prevalence of endogenous CD34+ adipose stem cells predicts human fat graft retention in a xenograft model,” *Plast. Reconstr. Surg.*, vol. 132, no. 4, pp. 845–858, 2013, doi: 10.1097/PRS.0b013e31829fe5b1.

[38] A. Scherberich, “A familiar stranger: CD34 expression and putative functions in SVF cells of adipose tissue,” *World J. Stem Cells*, vol. 5, no. 1, p. 1, 2013, doi: 10.4252/wjsc.v5.i1.1.

[39] R. A. Kopher, V. R. Penchev, M. S. Islam, K. L. Hill, S. Khosla, and D. S. Kaufman, “Human embryonic stem cell-derived CD34+ cells function as MSC progenitor cells,” *Bone*, vol. 47, no. 4, pp. 718–728, 2010, doi: 10.1016/j.bone.2010.06.020.

[40] B. C. Bellagamba, P. B. Grudzinski, P. B. Ely, P. D. J. H. Nader, N. B. Nardi, and L. Da Silva Meirelles, “Induction of expression of CD271 and CD34 in mesenchymal stromal cells cultured as spheroids,” *Stem Cells Int.*, vol. 2018, 2018, doi: 10.1155/2018/7357213.

[41] L. Da Silva Meirelles *et al.*, “Cultured Human Adipose Tissue Pericytes and Mesenchymal Stromal Cells Display a Very Similar Gene Expression Profile,” *Stem Cells Dev.*, vol. 24, no. 23, pp. 2822–2840, 2015, doi: 10.1089/scd.2015.0153.

[42] R. Shah *et al.*, “Gene profiling of human adipose tissue during evoked inflammation in vivo,” *Diabetes*, vol. 58, no. 10, pp. 2211–2219, 2009, doi: 10.2337/db09-0256.

[43] S. Hörl *et al.*, “CD146 (MCAM) in human cs-DLK1−/cs-CD34+ adipose stromal/progenitor cells,” *Stem Cell Res.*, vol. 22, pp. 1–12, 2017, doi: 10.1016/j.scr.2017.05.004.

[44] Y. Wang *et al.*, “Relative contributions of adipose-resident CD146+ pericytes and CD34+

adventitial progenitor cells in bone tissue engineering," *npj Regen. Med.*, vol. 4, no. 1, 2019, doi: 10.1038/s41536-018-0063-2.

[45] Z. Wang and X. Yan, "CD146, a multi-functional molecule beyond adhesion," *Cancer Lett.*, vol. 330, no. 2, pp. 150–162, 2013, doi: 10.1016/j.canlet.2012.11.049.

[46] L. Zimmerlin *et al.*, "Stromal vascular progenitors in adult human adipose tissue," *Cytom. Part A*, vol. 77, no. 1, pp. 22–30, 2010, doi: 10.1002/cyto.a.20813.

[47] P. Ercal, G. G. Pekozer, O. Z. Gumru, G. T. Kose, and M. Ramazanoglu, "Influence of STRO-1 selection on osteogenic potential of human tooth germ derived mesenchymal stem cells," *Arch. Oral Biol.*, vol. 82, no. March, pp. 293–301, 2017, doi: 10.1016/j.archoralbio.2017.06.028.

[48] G. Lin *et al.*, "Tissue distribution of mesenchymal stem cell marker stro-1," *Stem Cells Dev.*, vol. 20, no. 10, pp. 1747–1752, 2011, doi: 10.1089/scd.2010.0564.

[49] S. Mohamed-Ahmed *et al.*, "Adipose-derived and bone marrow mesenchymal stem cells: A donor-matched comparison," *Stem Cell Res. Ther.*, vol. 9, no. 1, pp. 1–15, 2018, doi: 10.1186/s13287-018-0914-1.

[50] Y. Miyata, M. Otsuki, S. Kita, and I. Shimomura, "Identification of Mouse Mesenteric and Subcutaneous in vitro Adipogenic Cells," *Sci. Rep.*, vol. 6, no. October 2015, pp. 1–14, 2016, doi: 10.1038/srep21041.

[51] P. C. Baer *et al.*, "Comprehensive phenotypic characterization of human adipose-derived stromal/stem cells and their subsets by a high throughput technology," *Stem Cells Dev.*, vol. 22, no. 2, pp. 330–339, 2013, doi: 10.1089/scd.2012.0346.

[52] Q. Li, L. J. Qi, Z. K. Guo, H. Li, H. B. Zuo, and N. N. Li, "CD73+ adipose-derived mesenchymal stem cells possess higher potential to differentiate into cardiomyocytes in vitro," *J. Mol. Histol.*, vol. 44, no. 4, pp. 411–422, 2013, doi: 10.1007/s10735-013-9492-9.

[53] Z. Pan *et al.*, "CD90 serves as differential modulator of subcutaneous and visceral adipose-derived stem cells by regulating AKT activation that influences adipose tissue and metabolic homeostasis," *Stem Cell Res. Ther.*, vol. 10, no. 1, pp. 1–18, 2019, doi: 10.1186/s13287-019-1459-7.

[54] M. C. Mitterberger *et al.*, "DLK1(PREF1) is a negative regulator of adipogenesis in CD105+/CD90+/CD34+/CD31-/FABP4- adipose-derived stromal cells from subcutaneous abdominal fat pats of adult women," *Stem Cell Res.*, vol. 9, no. 1, pp. 35–48, 2012, doi: 10.1016/j.scr.2012.04.001.

[55] Y.-K. Kim, H. Nakata, M. Yamamoto, M. Miyasaka, S. Kasugai, and S. Kuroda, "Osteogenic Potential of Mouse Periosteum-Derived Cells Sorted for CD90 In Vitro and In Vivo," *Stem Cells Transl. Med.*, vol. 5, no. 2, pp. 227–234, 2016, doi: 10.5966/sctm.2015-0013.

[56] S. J. Huang *et al.*, "Adipose-derived stem cells: Isolation, characterization, and differentiation potential," *Cell Transplant.*, vol. 22, no. 4, pp. 701–709, 2013, doi: 10.3727/096368912X655127.

[57] P. C. Baer, "Adipose-derived mesenchymal stromal/stem cells: An update on their phenotype in vivo and in vitro," *World J. Stem Cells*, vol. 6, no. 3, p. 256, 2014, doi: 10.4252/wjsc.v6.i3.256.

[58] J. R. Ingram *et al.*, “PD-L1 is an activation-independent marker of brown adipocytes,” *Nat. Commun.*, vol. 8, no. 1, 2017, doi: 10.1038/s41467-017-00799-8.

[59] N. D. Frank, M. E. Jones, B. Vang, and C. Coeshott, “Evaluation of reagents used to coat the hollow-fiber bioreactor membrane of the Quantum® Cell Expansion System for the culture of human mesenchymal stem cells,” *Mater. Sci. Eng. C*, vol. 96, no. March 2018, pp. 77–85, 2019, doi: 10.1016/j.msec.2018.10.081.

Appendix

Appendix 1.

Antibody mixture guide used in this experiment.

CD36 (BUV395) FMO *Brilliant Stain Buffer- 35,05 µl* *CD34 (BUV496)- 2 µl* *CD248 (BUV737)- 2 µl* *CD200 (BB515)- 2 µl* *CD271 (BB700)- 2 µl* *CD274 (PE-CF594)- 1,7 µl* *CD146 (PE-Cy7)- 1,25 µl* *Stro-1 (APC)- 4 µl*	**CD34 (BUV496) FMO** *Brilliant Stain Buffer- 35,35 µl* *CD36 (BUV395)- 1,7 µl* *CD248 (BUV737)- 2 µl* *CD200 (BB515)- 2 µl* *CD271 (BB700)- 2 µl* *CD274 (PE-CF594)- 1,7 µl* *CD146 (PE-Cy7)- 1,25 µl* *Stro-1 (APC)- 4 µl*	**CD248 (BUV737) FMO** *Brilliant Stain Buffer- 35,35 µl* *CD34 (BUV496)- 2 µl* *CD36 (BUV395)- 1,7 µl* *CD200 (BB515)- 2 µl* *CD271 (BB700)- 2 µl* *CD274 (PE-CF594)- 1,7 µl* *CD146 (PE-Cy7)- 1,25 µl* *Stro-1 (APC)- 4 µl*
CD200 (BB515) FMO *Brilliant Stain Buffer- 35,35 µl* *CD34 (BUV496)- 2 µl* *CD248 (BUV737)- 2 µl* *CD36 (BUV395)- 1,7 µl* *CD271 (BB700)- 2 µl* *CD274 (PE-CF594)- 1,7 µl* *CD146 (PE-Cy7)- 1,25 µl* *Stro-1 (APC)- 4 µl*	**CD271 (BB700) FMO** *Brilliant Stain Buffer- 35,35 µl* *CD34 (BUV496)- 2 µl* *CD36 (BUV395)- 1,7 µl* *CD248 (BUV737)- 2 µl* *CD200 (BB515)- 2 µl* *CD274 (PE-CF594)- 1,7 µl* *CD146 (PE-Cy7)- 1,25 µl* *Stro-1 (APC)- 4 µl*	**CD274 (PE-CF594) FMO** *Brilliant Stain Buffer- 35,05 µl* *CD34 (BUV496)- 2 µl* *CD36 (BUV395)- 1,7 µl* *CD248 (BUV737)- 2 µl* *CD200 (BB515)- 2 µl* *CD271 (BB700)- 2 µl* *CD146 (PE-Cy7)- 1,25 µl* *Stro-1 (APC)- 4 µl*
CD146 (PE-Cy7) FMO *Brilliant Stain Buffer- 34,6 µl* *CD36 (BUV395)- 1,7 µl* *CD34 (BUV496)- 2 µl* *CD248 (BUV737)- 2 µl* *CD200 (BB515)- 2 µl* *CD271 (BB700)- 2 µl* *CD274 (PE-CF594)- 1,7 µl* *Stro-1 (APC)- 4 µl*	**Stro-1 (APC) FMO** *Brilliant Stain Buffer- 37,35 µl* *CD36 (BUV395)- 1,7 µl* *CD34 (BUV496)- 2 µl* *CD248 (BUV737)- 2 µl* *CD200 (BB515)- 2 µl* *CD271 (BB700)- 2 µl* *CD274 (PE-CF594)- 1,7 µl* *CD146 (PE-Cy7)- 1,25 µl*	**Stained sample (Panel 1)** *Brilliant Stain Buffer- 33,35 µl* *CD36 (BUV395)- 1,7 µl* *CD34 (BUV496)- 2 µl* *CD248 (BUV737)- 2 µl* *CD200 (BB515)- 2 µl* *CD271 (BB700)- 2 µl* *CD274 (PE-CF594)- 1,7 µl* *CD146 (PE-Cy7)- 1,25 µl* *Stro-1 (APC)- 4 µl*
CD201 (BUV395) FMO *FBS- 46 µl* *CD73 (FITC)- 1 µl* *CD90 (Percp-cy5.5)- 1 µl* *CD105 (PE-CF594)- 1 µl* *CD166 (Alexa Fluor®647)- 1 µl*	**CD73 (FITC) FMO** *FBS- 46 µl* *CD201 (BUV395)- 1 µl* *CD90 (Percp-cy5.5)- 1 µl* *CD105 (PE-CF594)- 1 µl* *CD166 (Alexa Fluor®647)- 1 µl*	**CD90 (Percp-cy5.5.) FMO** *FBS- 46 µl* *CD73 (FITC)- 1 µl* *CD201 (BUV395)- 1 µl* *CD105 (PE-CF594)- 1 µl* *CD166 (Alexa Fluor®647)- 1 µl*
CD105 (PE-CF594) FMO *FBS- 46 µl* *CD73 (FITC)- 1 µl* *CD201 (BUV395)- 1 µl* *CD90 (Percp-cy5.5)- 1 µl* *CD166 (Alexa Fluor®647)- 1 µl*	**CD166 (Alexa Fluor®647) FMO** *FBS- 46 µl* *CD73 (FITC)- 1 µl* *CD201 (BUV395)- 1 µl* *CD90 (Percp-cy5.5)- 1 µl* *CD105 (PE-CF594)- 1 µl*	**Stained sample (Panel 2)** *FBS- 45 µl* *CD73 (FITC)- 1 µl* *CD201 (BUV395)- 1 µl* *CD90 (Percp-cy5.5)- 1 µl* *CD105 (PE-CF594)- 1 µl* *CD166 (Alexa Fluor®647)- 1 µl*

Appendix 2.
Example of the population tree view. P1 in Panel 1 (weakly expressed markers)